Next Generation Flood Modelling using 3Di: A Case Study in Taiwan

Ruben Dahm*
Catchment Hydrology Department
Deltares
Delft, The Netherlands

Chih-Tsung Hsu
High Performance Computing Division
National Center for High-performance Computing
Hsinchu, Taiwan

Ho-Cheng Lien
High Performance Computing Division
National Center for High-performance Computing
Hsinchu, Taiwan

Che-Hao Chang
Civil Engineering Department
National Taipei University of Technology
Taipei, Taiwan

Geert Prinsen
Catchment Hydrology Department
Deltares
Delft, The Netherlands

* Corresponding author's e-mail: ruben.dahm@deltares.nl

ABSTRACT

This paper explores the application of new flood modelling software with sub-grid and quad tree techniques; 3Di. The software is capable of using high resolution LIDAR based elevation data as input to the flood model while achieving run times which are significantly faster than conventional flood models. 3Di has been successfully applied in the Netherlands in polder areas to model pluvial flooding and flooding due to dike breaches in relatively flat areas. In this study, the 3Di application of the Mei-Fu drainage area in Taiwan is compared with an existing SOBEK 1D2D model for the Typhoon Saola (2012) event. The results of the study show that 3Di is applicable to model floods in (semi-) tropical urban and rural areas with high rainfall intensities and short lead times. Flood extent and maximum observed water levels are reproduced quite well by the model and moreover, these results are achieved in significantly less run time than the currently applied SOBEK 1D2D model. 3Di presents the flood model results on the resolution of the underlying high-resolution DEM which allows realistic visualisation of these results. The results presented show the potential of 3Di in both planning analyses and real-time forecasting applications.

Keywords: Urban flooding; Flood modelling; 3Di; Sub-grid; Quad trees; Taiwan.

1. INTRODUCTION

Flood modelling and urban flood risk management receive increasing attention because of population growth and large economic values of areas vulnerable to flooding. In recent years large-scale flood disasters have occurred in Manila, Philippines (2013); Beijing, China (2012); New York, USA (2012); Bangkok, Thailand (2011); and Brisbane, Australia (2011), while cities like Jakarta, Indonesia and Ho Chi Minh City, Vietnam experience floods almost every year. In order to reduce

flood risk more insight in the detailed behaviour of urban drainage systems is needed. High-speed and high-resolution flood models can be useful in obtaining this insight and are often required for long-term strategic planning, short-term operation and flood forecasting purposes. High-resolution elevation data with many data points per m^2 are more and more available through airborne light detection and ranging technology (LIDAR). For example, in the Netherlands the first national digital elevation model (2003) had a horizontal point density of 1 elevation observation per 16 m^2. In 2012, the Dutch government finalised a national digital elevation model with a point density of 6-10 points per m^2, a vertical systematic error of 0.05 m and a stochastic error of 0.05 m [1]. DEMs derived from such detailed data are often preferred to DEMs derived from coarser data because of horizontal resolution, vertical accuracy and the possibility to distinguish and if required separate buildings, vegetation and ground level [2]. However, 1D2D simulations on grids with pixels of 1x1 m or smaller for large areas is computationally cumbersome, e.g. the computational speed of SOBEK reduces at approximately 1 million grid cells, or becomes impossible for many of the existing modelling suites. A decade ago this was not a real problem, since detailed DEMs for large areas were hardly available. Nowadays, elevation grids with pixels of 1x1 m or even smaller are available. When using pixels of 1x1 m SOBEK computational speed would already reduce when assessing a 2D study area of only ~1 km^2.

Techniques like sub-grid [3] and quad trees [4] were developed to use high resolution DEM information and to improve detailed 2D flood simulations. 3Di uses these solver techniques. It is capable of fully utilising the high resolution LIDAR based DEM data. This makes it possible to apply high resolution DEM data as input to a flood model while achieving run times which are significantly faster than conventional flood models. 3Di has been successfully applied in Dutch polder areas for modelling pluvial flooding and flooding due to dike breaches [5].

In this paper, we present a new flood modelling software 3Di, its application on the case study of the flooding in the Mei-Fu drainage area (Yilan province, Taiwan) due to Typhoon Saola (2012) and we compare the simulation results with those of an existing SOBEK 1D2D model.

2. 3DI: NEXT GENERATION FLOOD MODELLING

2.1. General introduction

3Di is a new software system developed in the Netherlands by the 3Di consortium consisting of Deltares, the Delft University of Technology, Nelen & Schuurmans consultancy and regional water authorities. 3Di combines four numerical methods in its solver [6]: the sub-grid method [3], bottom friction based on the concepts of roughness depth [6], the finite-volume staggered grid method for shallow water equations with rapidly varying flows just like the SOBEK modelling suite [7, 8] and quad tree techniques [4]. 3Di uses Cartesian grids with square grid cells which can be easily generated. We refer to [6] and [9] for a detailed explanation of the numerical backgrounds.

2.2. Sub-grid

The sub-grid technique is based on grids with different resolutions. For the computation of water levels and velocities the fine grid pixels are clustered into larger cells, as shown in Figure 1a in which $\zeta_{l,m,n}$ is the water level above the reference plane, $e_{i,j}$ is the bottom elevation above reference plane, and $\Omega_{l,m,n}$ the hierarchical quad tree ordering. 3Di is constructing and using a table describing the relation between water level and volume for the large cell, based on the information of the detailed DEM. Hence, detailed information is aggregated and used when solving the 2D shallow water equations. Also the friction information available on the detailed DEM is aggregated to the larger cell, resulting in a friction depending on water depth taking into account the specified local friction variations.

2.2. Quad tree

Another aspect of 3Di is the use of quad trees, i.e. the grid cells used in the computation are not of constant size. The cell size is small on locations where large detail is required and large where this is not needed. Local grid refinements are made by recursively splitting cells in 4

quadrants, maintaining the orthogonality of the grid. In 3Di, the minimum and maximum cell size to be used in the computations must be specified. The software will generate a quad tree grid as shown in Figure 1b. In areas where the difference between the highest elevation and the lowest elevation from the detailed DEM is small, 3Di will generate larger cells. Also manual input and correction is possible, using polylines to define areas which need refinement.

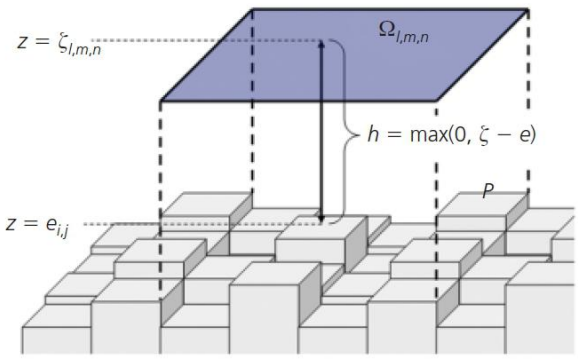

Figure 1a: Example of sub-grid [6].

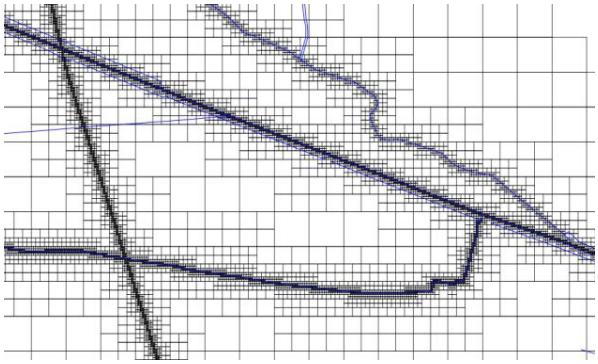

Figure 1b: Example of quad trees.

3. CASE STUDY: FLOODING IN MEI-FU DUE TO TYPHOON SAOLA

3.1. Study area

The case study area of Yilan County is located in the northeast of Taiwan. This study focusses on the Mei-Fu drainage area located in the downstream area of the Lanyang river basin as shown in Figure 2. The Mei-Fu drainage area includes three main urban drainage areas: Yilan City, Yilan County downtown and Zhuangwei. The total basin area is 1007.8 km^2 including 27.9 km^2 of the Mei-Fu drainage area. The Mei-Fu drainage system discharges to the Yiland river close to its confluence with the Lanyang river.

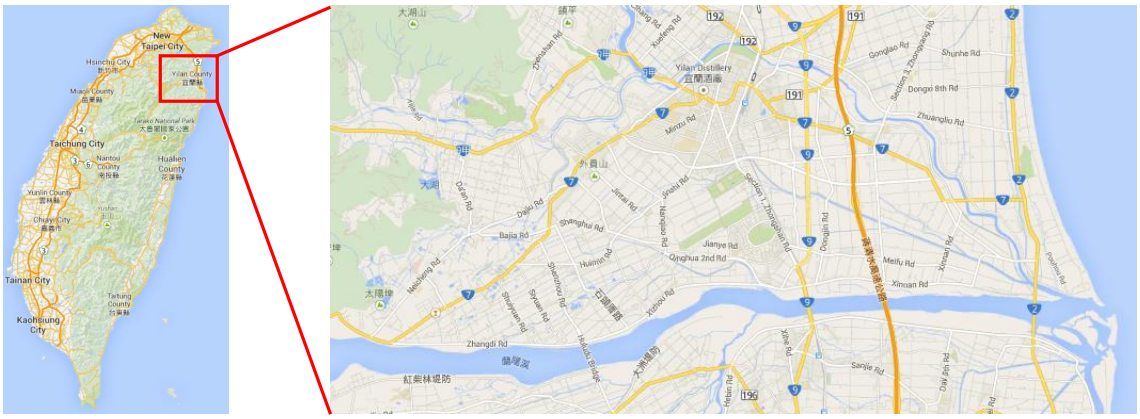

Figure 2: Location of Mei-Fu drainage area in Yilan county, north-eastern Taiwan.

3.2. Typhoon Saola

Taiwan is regularly hit by typhoons with torrential rains causing pluvial and fluvial flooding, landslides and economic damage. In 2012, Yilan County and Lanyang river basin were hit by Typhoon Saola from July 31 to August 3. Typhoon Saola resulted in five casualties and more than 1000 people were evacuated from mountainous villages. It caused damages at Taoyuan airport, disrupting of schools and businesses. Agricultural losses alone were estimated at some 27 million US$ [10]. The total accumulated rainfall at Taipingshan gauge station in the upstream catchment of Lanyang River is about 1922 mm. In Mei-Fu area, the rainfall was considerably lower, about 490 mm in five days. The maximum average hourly rainfall in Mei-Fu during Typhoon Saloa was 37 mm/hr. The Mei-Fu area was also affected by the high rainfall in the Lanyang river basin since this

caused high water levels in Lanyang river and backwater effect into the Mei-Fu drainage system. Post-disaster data of Typhoon Saola was collected afterwards. The data consists of 35 maximum flood depth observations in the area between the North-South directed railway and the Mei-Fu canal. The locations are indicated in Figure 3. When comparing these maximum flood depths to the 1x1 m DEM which was used in this study, it was found that:

- 2 observations are located outside the detailed DEM;
- 1 observation is located in a canal and for that reason discarded. This erroneous location might be due to a small shift in geo-referencing of either the location or the spatial elevation data;
- 6 observations are discarded since the sum of the flood depth and the local elevation results in an unrealistic water level.

This reduced the final set of observation locations used in this case study to 26 locations. These observations are compared to the simulation results of both SOBEK and 3Di.

Figure 3: Location of observation points in Mei-Fu area positioned on top of the 1x1 m DEM.

3.3. Existing model: SOBEK 1D2D

The Water Resources Agency within the Ministry of Economic Affairs has been using the Deltares SOBEK modelling suite [8] for flood modelling of various regions in Taiwan for more than 10 years already. The Taiwanese National Center for High Performance Computing (NCHC) developed a SOBEK application for Lanyang river and Mei-Fu area see Figure 4. This SOBEK model uses the rainfall-runoff, the 1D channel flow including structure control and the 1D2D inundation modules. The rainfall-runoff schematisation uses the Sacramento rainfall-runoff concept [11] and the NWRW urban runoff concept [12]. The distributed rainfall pattern of Typhoon Saola was averaged into 21 different time series. Each of the rural and urban sub-catchments was linked with one of these rainfall time series. The SOBEK 1D Flow model consists of over 800 cross-sections, and 14 (control) structures. Typical Manning roughness specified in the Mei-Fu drainage canals and pipe system is n=0.012 $s.m^{-1/3}$ and n=0.025 $s.m^{-1/3}$ respectively. The SOBEK 1D2D model component consists of 5 grids with a pixel size of 10x10 m (2 grids) or 20x20 m (3 grids). The 1D2D roughness is specified using the White-Colebrook formula with Nikuradse equivalent roughness values of K_n=0.8 m for the 20x20 m grids and K_n=10 m for the 10x10 m grids. The detailed grids represent areas with high urbanization rates while the coarser grids represent the rural area in the basin.

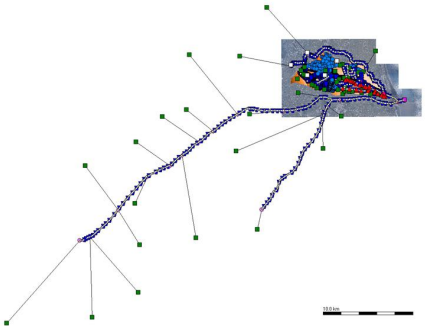

Figure 4a: Schematisation of Lanyang river basin.

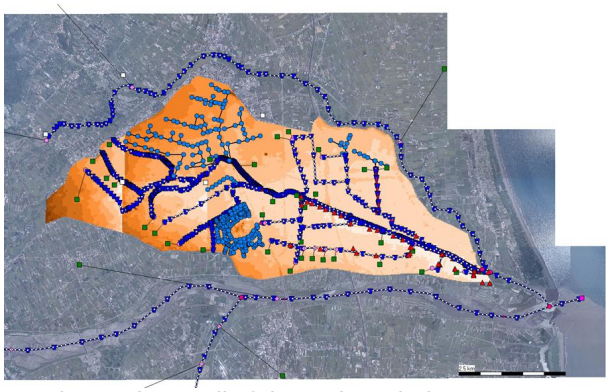

Figure 4b: Detail of the Mei-Fu drainage area.

3.3. 3Di model set up

3.3.1. Distributed rainfall-runoff

The distributed rainfall-runoff model in 3Di takes into account loss terms as interception, evaporation and infiltration. The 3Di development team implemented a rural rainfall-runoff concept in 3Di and is working on a distributed hydrology component which is suitable for international (urban) application. To account for differences in infiltration we distinguished pervious and impervious areas in the Mei-Fu basin. Based on the land use, soil map and the FAO guidelines [13] a maximum infiltration rate of 120 mm/day was applied for the pervious area. A default constant thickness of interception layer of 2.5 mm was applied, although 3Di is capable of using a spatial distribution of interception e.g. based on land use.

3.3.2. Digital Elevation Model

For the construction of the DEM grid of the Mei-Fu basin we used a 1x1 m resolution elevation model. The resulting DEM grid contains approximately 27.86 million grid pixels. Next, a separate 2D DEM grid layer was constructed representing the major drainage canals of the Mei-Fu area using the layout and cross-section information included in the SOBEK 1D network. A similar technique was applied to build a grid layer for the smaller urban pipes in the Mei-Fu basin although this results in a slight overestimation of the maximum wetted area. Including these smaller drainage canals in the DEM of the 3Di model is expected to improve the simulation of the overland runoff processes from the catchment surface to the main drainage canals. The separate grid layers were integrated to a final DEM grid used for the 3Di model. This DEM grid consists of 0.54 million grid pixels and includes both the main drainage canals as the smaller pipes network and they are 'burned' into the detailed 1x1 m grid.

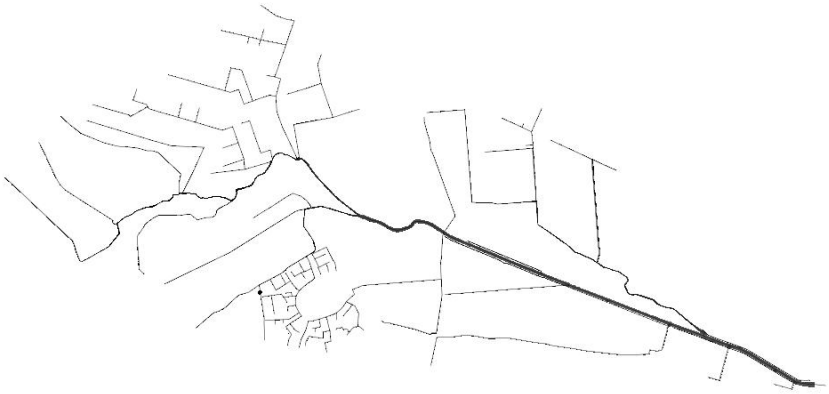

Figure 5: Grid layer of main drainage canals and smaller pipe network.

We used the land use map to derive spatially distributed roughness values. Agriculture (60%), construction land (16%) and transportation (11%) are the major land use categories in Mei-Fu drainage area. Manning's n roughness values are based on literature [14] and typically between n=0.025 and n=0.055 $s.m^{-1/3}$.

3.3.3. External forcing

The external forcing applied to the 3Di model includes a distributed rainfall time series and a 2D downstream discharge boundary. The rainfall time series is spatially applied over the Mei-Fu area. Figure 6 shows an example of the rainfall grid on top of the 3Di DEM where dark blue indicates higher rainfall intensities.

The discharge boundary is located downstream of Mei-Fu canal. The downstream boundary condition of the 3Di model is derived from the SOBEK results by taking the simulated discharge over the downstream outlet structure. This has to be done, since 3Di does not yet includes 1D flow structures. From the SOBEK simulation results it is seen that the outlet is blocked for about 14 hours in the night of August 2-3. This is either direct backwater effect, blocking the downstream outlet structure of Mei-Fu area, or manual operation of the structure closing it off in that period.

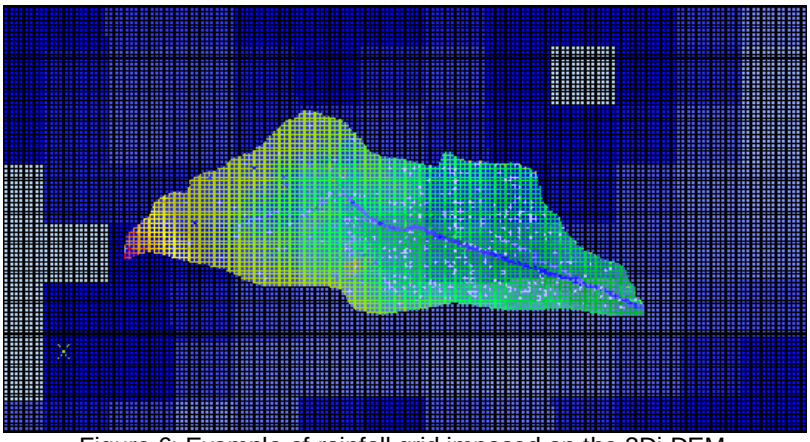

Figure 6: Example of rainfall grid imposed on the 3Di DEM.

3.3.4. Detailing quad trees

The 3Di algorithm is capable of automatic deriving elevated elements in the DEM. In a flat polder area such as in the Netherlands this routine is a sound approach to derive the quad trees. A maximum elevation difference between two quad trees of e.g. 0.5 m would guarantee that elevated line elements blocking the flow will be taken into account. However, in the Mei-Fu basin there is a natural difference in elevation of approximately 17 m over a range of 11 km. Due to the slope in the basin and the detailed 1x1 m information, a maximum elevation difference like 0.5 m between two quad trees is easily met. This will most likely result in a quad tree grid on the lowest level specified without making use of this novel approach. Next to automatic derivation of elevated elements, 3Di also allows users to generate polylines at which location 3Di is forced to use the lowest level specified. In this case study we used this method and included the railway and all major roads east of the railway which divides the drainage area in half in a north-south direction. Additionally, the major canals are included in this polyline.

3.3.5. Quad tree settings

Different quad tree cell sizes have been applied and both uniform and non-uniform (spatially refined) quad tree grids were tested. Due to the application of a rainfall grid directly to the quad tree, it is currently advised to use a grid which is as uniform as possible. This fits the numerical processes involved in rainfall runoff modelling better since relatively small volumes (layers) of rainfall water covering all grid cells dominate the flow processes. Furthermore, tests showed that when the quad tree grid cells are taken too small, this leads to a decrease in runoff volume. This is explainable since using smaller grid cell sizes results in more water stored on land due to local depressions of the surface elevation. Using larger grid cell sizes diminishes this effect. On the other hand, when the quad tree grid cells are taken too large, this leads to problems with the representation of the main canals and elevated line elements. Therefore, we applied a uniform quad tree grid with cell sizes 160x160 m except for the polyline locations where grid cells of at least 5x5 m, 10x10 m, 20x20 m, or 40x40 m were applied. These pixel sizes are based on the width of the main canals and on elevated line elements that might temporarily block the flow and redirect it before being overflow, e.g. a railway and roads.

The DEMs used in the SOBEK modelling count up to 186830 pixels, with 25.2% ‘no value’ pixels and 139672 pixels with elevation data. For the 3Di application, the 1x1 m sub-grid contains 10320x4860 = 50155200 pixels with 44.4% of ‘no value’ pixels and 27863903 pixels with elevation data. The 1x1 m DEM used by 3Di increases the number of pixels in comparison to the SOBEK simulation with a factor 200. However, 3Di uses the sub-grid and quad tree techniques which effectively can reduce the number of grid cells again depending on the chosen options. In this study we applied 4 coarse grids. Using the minimum pixel size in the quad tree ordening (Γ or ‘gridspace’) and lmax as the number of levels in the quad tree we defined four grids, see Table 1 and Figure 7.

Table 1 Grids in 3Di computations

Grid	Option minimum cell size (Γ)	Maximum nr of levels (lmax)	Number of active cells
Grid 1	40	3	2788
Grid 2	20	4	5757
Grid 3	10	5	12201
Grid 4	5	6	26089

Using these definitions, the maximum grid cells size is 160x160 m for all grids, while the minimum grid cell size decreased from 40 to 5. 3Di decreases the number of cells with a factor of 1000 to 10000 compared to the 1x1 m DEM. Although grid 1 is expected not to incorporate all flow blocking elements correctly, we included it for demonstration purposes. Note that the 3Di number of active grid cells is also less than in SOBEK.

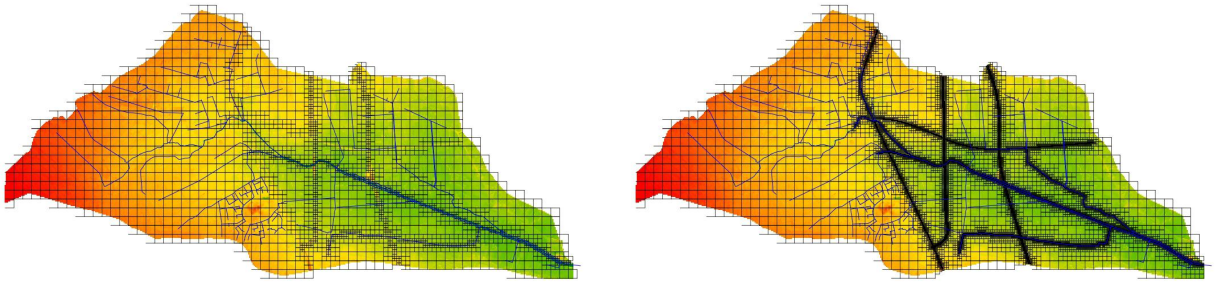

grid 1: Γ = 40 and l_{max} = 3 grid 4: Γ = 5 and l_{max} = 6

Figure 7: Example of the quad trees of grid 1 and 4.

4. RESULTS AND DISCUSSION

Figure 8 illustrates the SOBEK and 3Di computed flood extent for different times between July 30 and 2nd of August 2012, 23:00 o'clock. The flood depth is indicated in blue, with light blue being low inundation depth, and deep dark blue high flood depths. Unfortunately, the SOBEK interface shows also a lot of black spots (for the velocity vectors) for (almost) dry cells and these should be neglected. We present the results of the 3Di calculation using the grid with at least 40x40 m cell size in the Mei-Fu area. The propagation of the flood can be monitored from the figures with results at intermediate times. It seems that there is some small flooding on July 31 and August 1, but the large flooding is at August 2 after heavy rainfall and flood propagation from the northwest to the east. The results show that in these computations in 3Di the flooding starts earlier than in SOBEK. The different way of rainfall-runoff modelling in 3Di using rainfall directly on the grid might explain this. But since we not have the exact timing, we do not know whether 3Di is better than SOBEK in this respect or not. At the end of the simulation, 3Di shows a more or less continuous flood extent where the SOBEK result shows a similar area, but the flooded area is not completely connected. There are some isolated spots of flooding. Probably SOBEK is, due to using 1 average surface elevation level per cell where 3Di is using a level-volume relation, more sensitive for local depressions. The distributed forcing of rainfall instead of a lumped rainfall-runoff concept might also cause differences in flood extent.

Table 2 shows that the differences between 3Di and the observations are smaller (closer to zero) than the differences between SOBEK and the observed maximum flood depth. Stelling (2012) writes that the quad tree scaling using Γ and lmax only has a limited impact on the 3Di results. That is also reflected in the results we find: the absolute average error and standard deviation for the 4 grids used in 3Di are almost the same. We also find that the SOBEK computation time is larger than the computation times using grid 1 to 3. Only with the most detailed grid 4 (with minimum 5x5 m cell size) 3Di takes more time than the SOBEK computation. Probably the application of the distributed rainfall-runoff model explains why 3Di computation using grid 4 is slower than SOBEK. On the other hand, the 3Di results are generally closer to the observations than the SOBEK results. These results are in line with 3Di applications on Dutch polder systems.

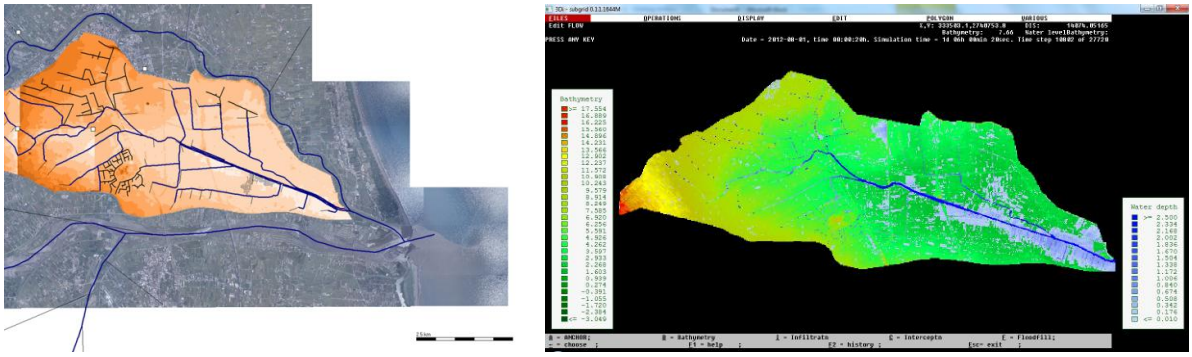

August 1, 00:00 AM

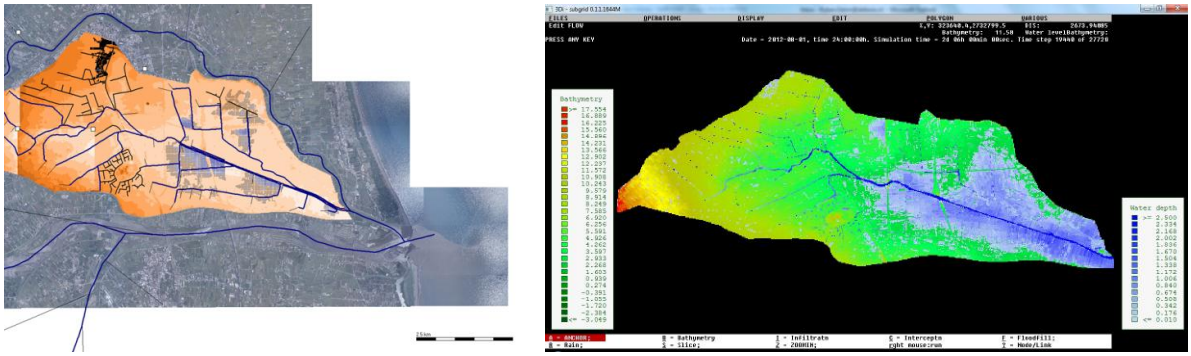

August 2, 00:00 AM

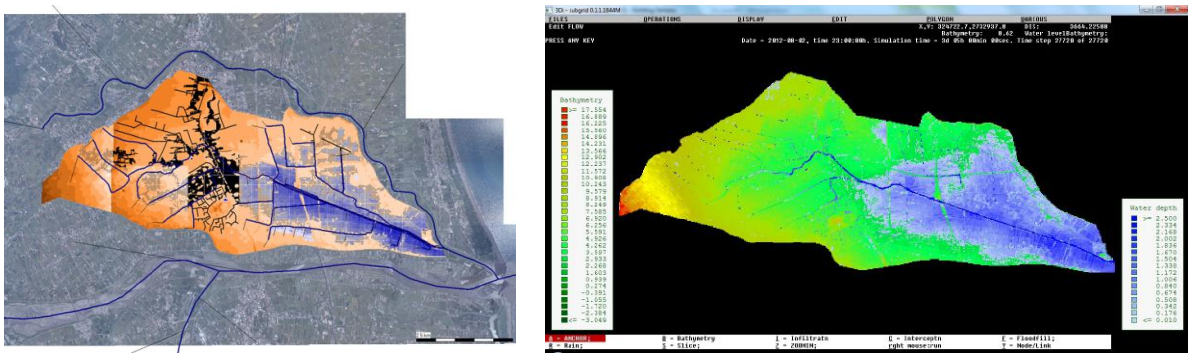

August 2, 23:00 PM

Figure 8a: Simulated flood extents of SOBEK 1D2D. Figure 8b: Simulated flood extents of 3Di.

Table 2: Computation times and performance

	Simulation time (s)	Active internal nodes	Abs. average error (m) compared with observations	Standard deviation (m)
SOBEK	6431.0	~ 136000	0.67	0.50
3Di grid 1	561.3	2788	0.54	0.39
3Di grid 2	1279.1	5757	0.54	0.39
3Di grid 3	3861.6	12201	0.54	0.39
3Di grid 4	13621.0	26809	0.54	0.39

It must be stated that comparing the results of SOBEK and 3Di is not straightforward, since the used DEM information is different. And for 3Di, the water level is calculated at a point using an interpolation relation between water level and the volume, based on detailed sub-grid data. To compare to the observations, we specified a 3x3 m area with the observation in the centre and

computed the average depth, since the coordinates of the observation location maybe less accurate than 1 m. The differences of the surface elevation between the SOBEK DEM and the 3Di averaged DEM are shown in Figure 9a. Black dots represent the SOBEK elevation; red lines represent the minimum and maximum elevation in the 3x3 m pixels at the observation location in the LIDAR DEM as used by 3Di. On average 3Di elevation at the observation locations is higher than the DEM used by SOBEK. Figure 9b shows the differences in maximum flood depth between SOBEK and the observations, and between 3Di and the observations, for the selected 26 observation locations. Again the black dots represent SOBEK results; red lines represent the results when using the minimum and maximum elevation in the 3x3 m pixels at the observation location, and the red dot represents 3Di results with average elevation.

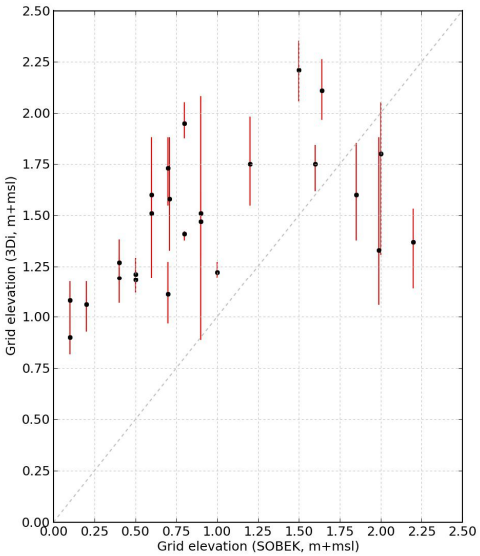

Figure 9a: Difference in elevation level of SOBEK DEM and 3Di averaged DEM.

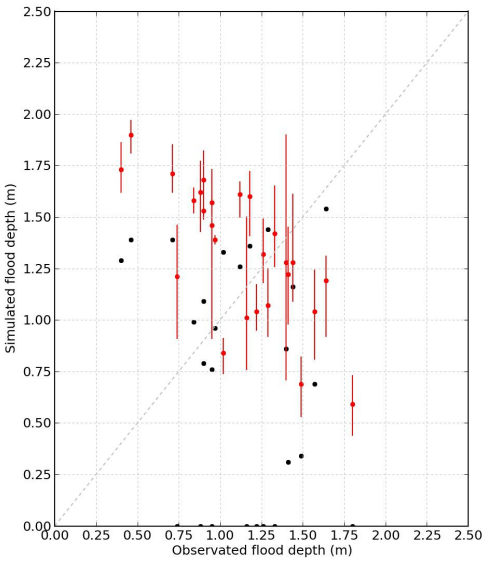

Figure 9b: Difference in observed and simulated maximum flood depth at 26 locations.

A satellite image of the flood was taken on August 2, 17:51PM (GMT+8). Both the SOBEK and 3Di simulated flood extents exceeding a threshold of 0.01 m flood depth are positioned on top of the satellite image see Figure 10. The satellite image is reproduced quite well in the south-eastern Mei-Fu area, but in the west and north-western urban area SOBEK computes inundations not visible on the satellite image. When comparing the 3Di flood extent with the satellite image, it matches quite well.

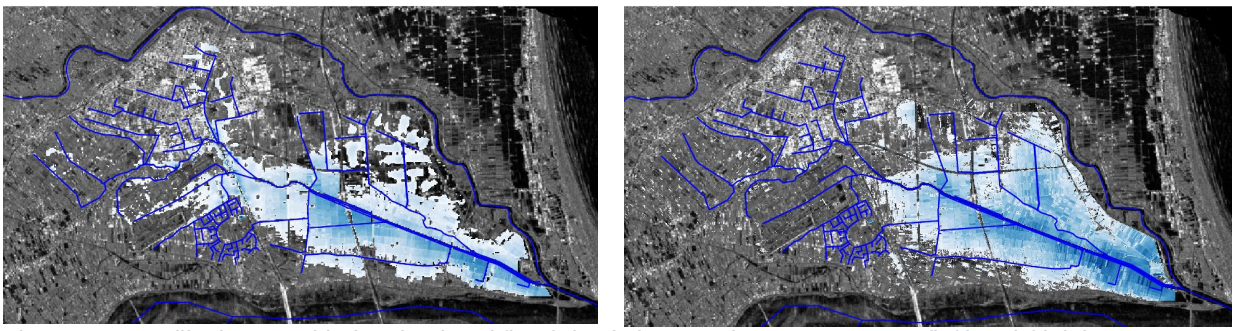

Figure 10: Satellite image with the simulated flood depth (>0.01 m) on top; SOBEK (left) 3Di (right).

Figure 11 shows the detail of 3Di results due to the fact the solver is capable of using LIDAR information in the flood simulation. This type of detailed visualisation could support decision makers when assessing flood risk mitigation measures or e.g. in an operational context.

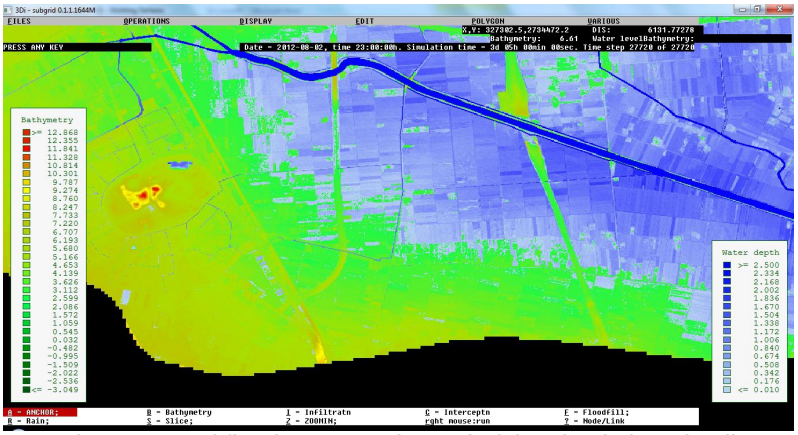

Figure 11: 3Di flood extent at the end of the simulation; detail

5. CONCLUSION

We applied 3Di for the Mei-Fu drainage area in Taiwan and compared the results with observations and simulations of an already existing SOBEK model. The Mei-Fu case study shows 3Di is capable of simulating extreme typhoon rainfall on a grid, where SOBEK had to be used using lumped rainfall-runoff concepts. Distributed rainfall requires more computation time than a lumped modelling approach, but still 3Di runs faster. A distributed rainfall-runoff modelling approach is more detailed and realistic (e.g. better representation of local upstream flooding). The differences in approach and schematisation will affect the comparison of results, but we believe that the general conclusion of a faster and more accurate 3Di remains valid. The 3Di sub-grid and quad tree techniques allow use of very detailed DEM data. This data is aggregated by 3Di and the detailed information is taken into account in the computations in a smart way. 3Di can use coarser numerical computation grids and compute faster, while still getting good results. The case study shows that 3Di is applicable for flood modelling in (semi-) tropical urban and rural areas with high rainfall intensities and short lead times. The flood model results are shown on the resolution of the underlying high-resolution DEM and this allows realistic visualisation.

Future 3Di developments are focussed on the integration of a 1D hydrodynamic urban flow module [9], coupling with the open-source RTC-Tools software [15] to include operational control of structures, development of a Delft-FEWS [16] 3Di adapter for operational flood forecasting, and web-cloud services to use 3Di on e.g. tablets and 3D visualisation techniques [5]. Including some of these developments in this case study is likely to improve the presented results.

This leads to the conclusion that 3Di is very promising: in this case study 3Di increased the number of elevation pixels used in the 2D flood modelling by a factor 200, while decreasing the number of active nodes by a factor 1000-10000. It runs faster than SOBEK, while at the same time the results are closer to the observed flood depths. The results presented show the potential of 3Di in view of flood modelling for flood risk management, forecasting and operational applications.

ACKNOWLEDGEMENTS

We thank the National Taipei University of Technology, National Centre for High Performance Computing in Hsinchu and Deltares, the Netherlands for funding this research. The authors thank Professor Stelling (formerly Delft University of Technology / National University Singapore) and Govert Verhoeven (Deltares) for discussions and assistance contributing to this study and paper.

REFERENCES

1. Algemeen Hoogtebestand Nederland (2013). Kwaliteitsdocument AHN2 [Quality guidance document].
2. Sanders, B. (2007). Evaluation of on-line DEMs for flood inundation modelling. *Advances in Water Resources.* 30(8): 1831–1843. doi: 10.1016/j.advwatres.2007.02.005.
3. Casulli, V (2009). A high-resolution wetting and drying algorithm for free-surface hydrodynamics. *International Journal for Numerical Methods in Fluids.* 60(4): 391–408.
4. Wang, J.P., Borthwick, A.G.L. and Eatock Taylor, R. (2004). Finite-volume type VOF method on dynamically adaptive quadtree grids. *International Journal for Numerical Methods in Fluids* 45(5): 485–508. doi: 10.1002/fld.712.
5. www.3di.nu/international/. Retrieved September 6, 2014.
6. Stelling, G.S. (2012). Quad tree flood simulations with sub-grid digital elevation models. *Institution of Civil Engineers (ICE) Proceedings - Water Management.* 165(WM10).
7. Stelling, G.S. and Duinmeijer, S.P.A. (2003). A staggered conservative scheme for every Froude number in rapidly varied shallow water flows. *International Journal for Numerical Methods in Fluids* 43(12): 1329–1354.
8. www.deltaressystems.com/hydro/product/108282/SOBEK-suite. Retrieved September 6, 2014.
9. Casulli V and Stelling GS (2013). A semi-implicit numerical model for urban drainage systems. *International Journal for Numerical Methods in Fluids* 73(6):600-614. doi/10.1002/fld.3817.
10. http://focustaiwan.tw/news/aeco/201208060044.aspx. Retrieved September 6, 2014.
11. Burnash, R.J.C., Ferral, R.L. and Mc.Guire, R.A. (1973). A generalized streamflow simulation system. Conceptual modelling for digital computers. Dept. of Water Resources, Sacramento.
12. NLingenieurs. (1978). Position paper Riolering. Technical report: 443, 599, 659, 660.
13. www.fao.org/docrep/s8684e/s8684e0a.htm. Retrieved September 6, 2014.
14. Maidment, D.R. (1993). Handbook of Hydrology, McGrawHill. ISBN 0-07-039732-5
15. oss.deltares.nl/web/RTC-tools. Retrieved September 6, 2014.
16. Werner, M., Schellekens, J., Gijsbers, P., van Dijk, M., van den Akker, O., Heynert, K. (2013). The Delft-FEWS flow forecasting system. *Environmental Modelling and Software 40:65-77.* http://dx.doi.org/10.1016/j.envsoft.2012.07.010.